Available online at www.sciencedirect.com
SCIENCE DIRECT®
Optics Communications 264 (2006) 482–487
OPTICS COMMUNICATIONS
www.elsevier.com/locate/optcom

Generation of a dark nonlinear focus by spatio-temporal coherent control

Haim Suchowski *, Dan Oron, Yaron Silberberg

Department of Physics of Complex Systems, Weizmann Institute of Science, Rehovot 76100, Israel

Received 10 November 2005; accepted 8 February 2006

Abstract

The transition probability of a two-photon absorption (TPA) process in atomic Cesium, excited by phase-controlled temporally focused ultrashort pulses is shown to be spatially modulated in a controlled manner. In particular, we demonstrate the generation of a dark nonlinear focus. By controlling the excitation pulse shape along the propagation coordinate we create a region in space where the TPA rate vanishes which is flanked by bright regions.

PACS: 32.80.Qk; 42.65.Ky

Keywords: Temporal focusing; Two-photon absorption; Coherent control

1. Introduction

A dark focus is a point in space which is a local zero in the amplitude of the electromagnetic field. Dark foci have been used for applications such as imaging [1] and trapping [2]. Here we present the concept of a dark nonlinear focus, i.e. a local zero in the transition probability of a multiphoton process. In contrast with linear processes, in a multiphoton process, a vanishing transition probability does not require that the field amplitude vanish. This is due to the fact that multiple paths leading to a multiphoton transition can destructively interfere [3]. Thus, spatial variation of the spectral phase of an ultrashort pulse driving a multiphoton process can suffice in generating a dark nonlinear focus, even when the field intensity is nonzero.

In order to spatially modulate the transition probability of a multiphoton absorption process, one needs to control ultrashort pulses both in space and in time. Whereas temporal manipulation of ultrashort pulses is by now an established technique [3–6], only few attempts at spatio-temporal control have been reported. Modulation of the temporal profile of ultrashort pulses by propagation in a resonant medium is perhaps the simplest form of such control [7], but is very limited in its applicability. True two-dimensional (2D) pulse shaping, utilizing a 2D spatial light modulator, has been used to control impulsive excitation of phonon-polaritons in a nonlinear crystal [8]. In this realization, the pulse shape varies along the transverse coordinate. Recently, we have utilized a combination of temporal focusing and standard Fourier domain pulse shaping, similar to the one used here, to control the axial response of a third-harmonic generation microscope [9].

In this work, we focus on spatio-temporal control of two-photon absorption (TPA) in an atomic gas, a narrow optical transition induced by a shaped broadband excitation pulse. This system has been extensively studied in the last few years [3,10–14]. In short, it was shown that the amount of TPA can be controlled by application of an appropriate spectral phase mask to the excitation pulse, due to interference between the multiple spectral paths leading to TPA excitation. In particular, for nonresonant TPA, the rate can vary between the maximal rate, achieved

* Corresponding author. Tel.: +972 8 9344035; fax: +972 8 9344109.
E-mail addresses: fehaim@wisemail.weizmann.ac.il (H. Suchowski), yaron.silberberg@weizmann.ac.il (Y. Silberberg).

0030-4018/$ - see front matter © 2006 Elsevier B.V. All rights reserved.
doi:10.1016/j.optcom.2006.02.064

using a transform-limited excitation pulse, and zero. The latter case was termed a "dark pulse" [3]. The same principle has also been applied to Raman transitions [4,15,16].

The spatial control of the TPA process in the present work is due to the excitation scheme which utilizes temporally focused shaped ultrashort pulses [9]. In short, temporal focusing [17–19] is a method of introducing dispersion of geometric origin, which varies with the propagation coordinate. A temporally focused ultrashort pulse is initially stretched, is compressed as it propagates, reaching its shortest duration (and highest peak intensity) at the temporal focal plane, and stretches again as it further propagates. The setup enabling the generation of temporally focused pulses consists of a diffraction grating, which is imaged by a telescope onto the sample. Incorporation of a spatial light modulator at the Fourier plane of the telescope enables to generate more complicated waveforms at the temporal focal plane with relative ease [9].

In the following, we first present in Section 2 a simple theoretical analysis of TPA induced by temporally focused pulses. The experimental setup enabling spatio-temporal control of the TPA rate is detailed in Section 3. The experimental results, showing the generation of a dark focal plane whose location is electronically controlled are presented in Section 4. A summary and conclusions are presented in Section 5.

2. Theory

2.1. Nonresonant TPA

We consider here the interaction of a weak ultrashort pulse with a two level system and follow the derivation of Meshulach and Silberberg [3] for nonresonant TPA. In this case, the nonresonant excited state population amplitude can be approximated by:

$$a_{\mathrm{f}}(\omega_{\mathrm{fg}}) \approx -\frac{1}{\hbar^2}\sum_n \frac{\mu_{\mathrm{f}n}\mu_{n\mathrm{g}}}{\omega_{n\mathrm{g}}-\omega_{\mathrm{fg}}/2} \times \int_{-\infty}^{\infty} \mathrm{d}\Omega E(\omega_{\mathrm{fg}}/2-\Omega)E(\omega_{\mathrm{fg}}/2+\Omega) \quad (1)$$

where ω_{fg} is the transition frequency, $E(\omega)$ is the pulse spectrum and the summation is taken over all the (far detuned) intermediate states. The two-photon transition probability can thus be controlled by tailoring the pulse spectral phase. It is maximized by the transform-limited pulse, i.e. the pulse having the minimum duration or a constant spectral phase $\Phi(\omega)$, and is unaffected by any antisymmetric spectral phase distribution around the the two-photon transition frequency $\omega_{\mathrm{fg}}/2$. Furthermore, the transition can be completely suppressed by careful arrangement of the phases to form complete destructive interference of all paths contributing to the excited state population. Thus, such "dark pulses" induce no net absorption.

In particular, it was shown [10] that a dark pulse can be achieved by applying a spectral phase filter in the form of a π spectral phase-step. Consider a pulse characterized by a sech spectrum of bandwidth $\Delta\omega$. Applying a π phase-step at spectral position shifted by δ from $\omega_{\mathrm{fg}}/2$ results in a field:

$$E(\omega_{\mathrm{fg}}/2+\Omega) = \mathrm{sech}\left(\frac{1.76\Omega}{\Delta\omega}\right)\exp\left[\mathrm{i}\frac{\pi}{2}\mathrm{sign}(\Omega-\delta)\right] \quad (2)$$

The TPA signal induced by this field vanishes when $\delta/\Delta\omega = \pm 0.31$, whereas for $\delta/\Delta\omega = 0$, corresponding to an antisymmetric spectral phase, the excited state population reproduces that achieved by a transform-limited pulse.

2.2. Temporal focusing

Temporal focusing is a process in which a chirped pulse propagates in a dispersive medium so that the chirp is removed and a transform-limited pulse is obtained at the temporal focus, in a process analogous to the spatial focusing of beam with a quadratic spatial phase induced by a lens. Since material dispersion is relatively weak and would lead to very slow temporal focusing, it is necessary to construct systems in which dispersion results from geometric origin, in order to achieve tight and controllable temporal focusing.

Optical devices based on angular dispersion, such as prisms and gratings, have been studied extensively in this context. This idea was first implemented by Treacy [21] for the compression of chirped pulses with diffraction gratings. The relation between angular dispersion and group-velocity dispersion (GVD) for several optical elements sequences had been studied by [21,22]. Such devices are employed for pulse stretching and compression, often in the context of short-pulse amplification.

By a combination of focusing and angular dispersive elements, one can indeed achieve large GVD over short distances. Martinez [22] analyzed such a system composed of a grating positioned at the front focal plane of a telescope with an angular magnification of $M = \frac{f_1}{f_2}$. This system introduces an optical chirp (i.e. quadratic spectral phase) which is given by

$$\frac{\mathrm{d}^2\Psi}{\mathrm{d}\Omega^2} = -\frac{w_l}{c}\left(\frac{\mathrm{d}\alpha}{\mathrm{d}\Omega}\right)^2 M^2 z \equiv 2\beta z \quad (3)$$

where Ψ is the total optical phase, $\frac{\mathrm{d}\alpha}{\mathrm{d}\Omega}$ is the angular dispersion of the grating, z is measured from the back spatial focal plane of the telescope, ω_l is the central spectrum value and $\Omega = \omega - \omega_l$. We have defined the chirp coefficient $\beta = -\frac{k}{2}\frac{\mathrm{d}\alpha^2}{\mathrm{d}\Omega}M^2$. One can see that the chirp is linearly dependent on z and can change sign from positive to negative values. The geometric chirp vanishes at the back focal plane at $z = 0$.

A transform-limited pulse which is introduced into this system emerges from the telescope greatly chirped, but it undergoes fast temporal focusing, and it reaches its transform-limited duration again at the back focal plane. This system was used recently to achieve scanningless depth resolved multiphoton microscopy [17] and to improve the contrast in line-scanning multiphoton microscopy [18,19].

Inserting a spatial light modulator (SLM) at the fourier plane of the telescope [6] results in a mapping of the temporal behavior into a spatial one, enabling the application of

an arbitrary spectral phase function to the pulse. In this experiment, we combine this with temporal focusing, and show how the properties of the temporal focus can be altered by pulse shaping. In particular, adding a quadratic spectral phase changes the position of the temporal focus relative to the spatial focus, as is obvious from Eq. (3).

2.3. Dark focus – theoretical treatment

Taking into consideration the fact that an antisymmetric spectral phase applied at the SLM does not influence the two-photon transition, we get that only the even part of the spectral phase can manipulate the spatial distribution of the TPA rate. There is an infinite choice of spectral phase functions $\Phi(\omega)$ which lead to generation of a dark pulse. In the following we analyze the spatial structures induced by such pulses, and in particular the spatial distribution of TPA near a temporal focus. We examine the particular case where $a_f(\omega_{fg}) = 0$ at $z = 0$, i.e. the case of dark nonlinear focus.

When choosing a phase function inducing a dark focus at $z = 0$, we choose an $E(\omega) = A(\omega)\exp(i\Phi(\omega))$ such that:

$$a_f(\omega_{fg}) = \int_{-\infty}^{\infty} d\Omega E(\omega_{fg}/2 - \Omega)E(\omega_{fg}/2 + \Omega) = 0 \tag{4}$$

examining this probability when we add a quadratic spectral phase, as is the case at $|z| > 0$, the electric field becomes $E(\omega) \rightarrow E(\omega)\exp(i\beta\omega^2 z)$. In this case, we get

$$a_f(\omega_{fg}, \beta) \approx \int_{-\infty}^{\infty} d\Omega E(\omega_{fg}/2 - \Omega)E(\omega_{fg}/2 + \Omega)\exp\left(2i\beta\Omega^2 z\right) \tag{5}$$

In the limit of small shifts from the temporal focal plane, i.e. $|\beta\Omega^2 z| \ll 1$ we can approximate this as:

$$a_f(\omega_{fg}, \beta) = \int_{-\infty}^{\infty} d\Omega E(\omega_{fg}/2 - \Omega)E(\omega_{fg}/2 + \Omega)\left(1 + 2i\beta\Omega^2 z\right) \tag{6}$$

By the definition of (Eq. (4)) the first term vanishes. The second term is simply a variance term, correlated with the spatial extent of the dark focus. The dark focus with the smallest spatial extent is obtained when the variance term of Eq. (6) is maximized. It is easy to see that this is obtained for the case of the π-step pulse, described in Eq. (2), as in this case the destructive interference is between contributions from the central part of the pulse spectrum and those from the outer parts. We therefore choose this particular shape to generate a dark focus in the following experiment.

Moreover, since these results are not affected by third-order dispersion (or, for that matter by any odd order dispersion) experienced by the pulse, the existence of the dark nonlinear focus is robust.

3. Experimental setup

In the experimental realization we observe the $6S_{1/2} - 8S_{1/2}$ two-photon transition of atomic cesium, at a wavelength of 411 nm. This transition is induced by 100 fs pulses centered at 822 nm, as shown schematically in Fig. 1(a). The two-photon transition amplitude is monitored by observing the 460 nm emission due to fluorescent decay via the $7P$ level to the ground state.

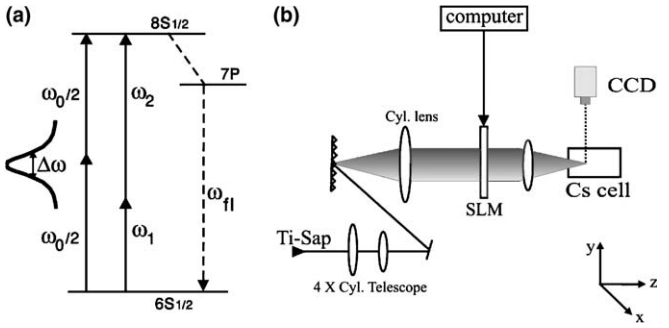

Fig. 1. (a) Schematic diagram of the energy levels of the $6S_{1/2} - 8S_{1/2}$ two-photon transition in atomic Cs. The excited state population amplitude is monitored by observing the spontaneous decay to the ground level through the $7P$ level. (b) The experimental setup, see text for details. The coordinate system is showed at the bottom right.

Our experimental system, schematically plotted in Fig. 1(b), consists of a Ti:Sapphire laser oscillator delivering 100 fs pulses at a repetition rate of 80 MHz. Pulses were spatially shrunk by an X4 cylindrical telescope along the horizontal (X) axis and directed at a 600 l/mm grating aligned perpendicular to the optical axis of a X10 telescope consisting of a 300 mm cylindrical lens and a 30 mm spherical achromat. This results in spatial focusing along the vertical (Y) direction [18,19], so that TPA is practically observed from a sheet lying in the X–Z plane. Care was taken to colocalize the temporal focal plane and the spatial focal plane. A programmable liquid crystal spatial light modulator (CRI SLM-128 Phase) was placed at the fourier plane of this telescope and used as a dynamic filter for spectral phase manipulation of the pulses. The shaped pulses were then directed into a Cs cell at a temperature of ~70°. We verified that at this temperature propagation effects due to the 6P resonance of Cs at 852 nm are negligible. The fluorescent decay through the 7P level at 460 nm was imaged from above onto a CCD camera (Mintron MTV-12V1 CCIR) using a $f = 25$ mm lens, and digitized on a computer.

4. Experimental results

Let us first consider the effect of chirp on TPA excitation with temporally focused pulses. Since a temporally focused beam experiences net second order dispersion away from the focus, this is merely expected to result in a shift of the temporal focal plane. To realize this experimentally we use the SLM to apply a variable amount of chirp to the excitation pulse. Shown in Fig. 2 are images, as grabbed from the CCD camera, for values of the dispersion ranging from $-10^4[fs^2]$ to $+10^4[fs^2]$, along with a schematic drawings of the applied spectral phase function. As can be seen, this indeed results in a shift of the peak TPA position along

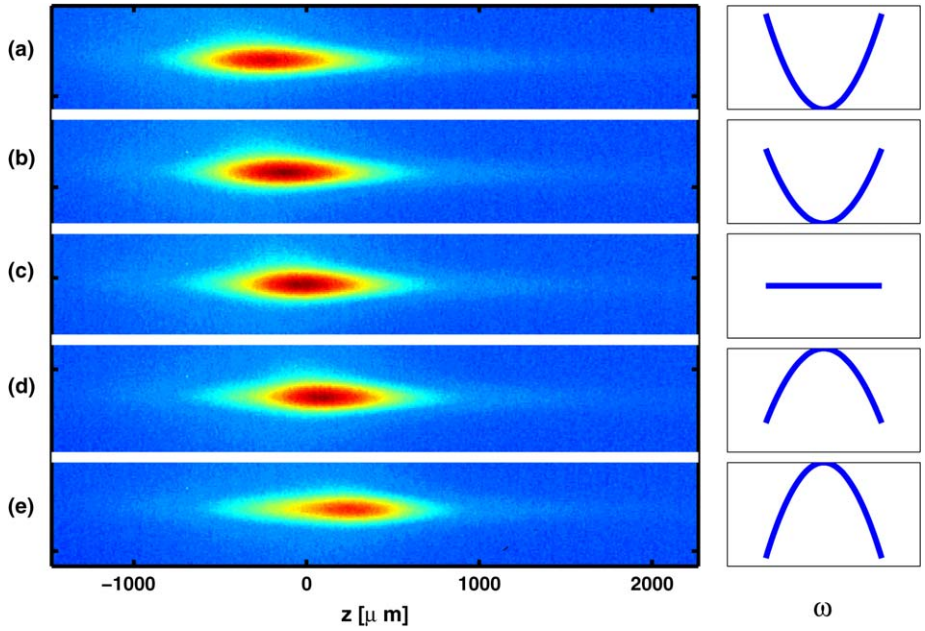

Fig. 2. The effect of GVD on the TPA spatial distribution. Shown for each image is a schematic of the spectral phase function applied on the SLM. Images correspond to GVD values ranging from (a) $-10^4[fs^2]$ to (e) $+10^4[fs^2]$. The net effect of the applied GVD is to move the location of the temporal focus along the propagation axis.

the propagation axis. The observed decrease in the peak TPA rate, as well as the peak asymmetry (with a tendency to the z = 0 position), for larger chirp are both due to the reduced overlap with the spatial focus (located at $z = 0$).

To generate a dark nonlinear focus, one has to apply a pulse shape generating a dark pulse at $z = 0$ on the SLM. Following the discussion of Section 2 we choose to use a π phase-step pulse as described in Eq. (2). In Fig. 3 we show the TPA images for several values of the π step location $\delta/\Delta\omega$. As expected, we see a high TPA signal for large values of $\pm\delta/\Delta\omega$, corresponding to a transform-limited pulse. The TPA almost vanishes at $z = 0$ for $\delta/\Delta\omega = \pm 0.31$, corresponding to a dark pulse at this location. Away from $z = 0$, however, the dispersion due to the temporal focusing destroys this delicate destructive interference effect, resulting in a finite TPA rate. Thus, the

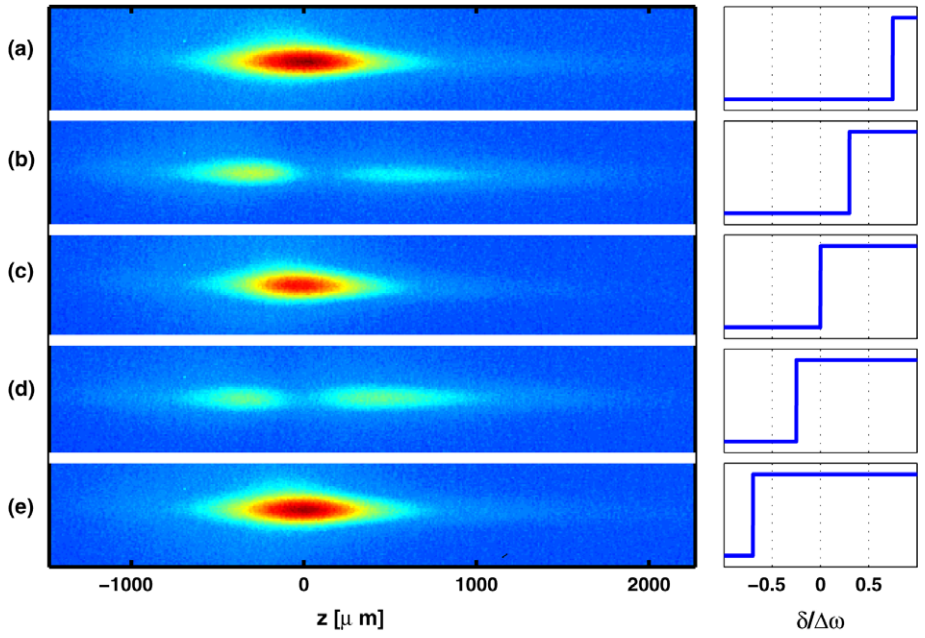

Fig. 3. The effect of a π phase-step on the TPA spatial distribution for several values of the step spectral location δ. Shown for each image is a schematic of the spectral phase function applied on the SLM. Images (a) and (e) denote a transform-limited pulse. For $\delta/\Delta\omega = \pm 0.31$ (b, d) a dark nonlinear focus appears at $z = 0$ for $\delta = 0$ and (c) the transform-limited result is reproduced.

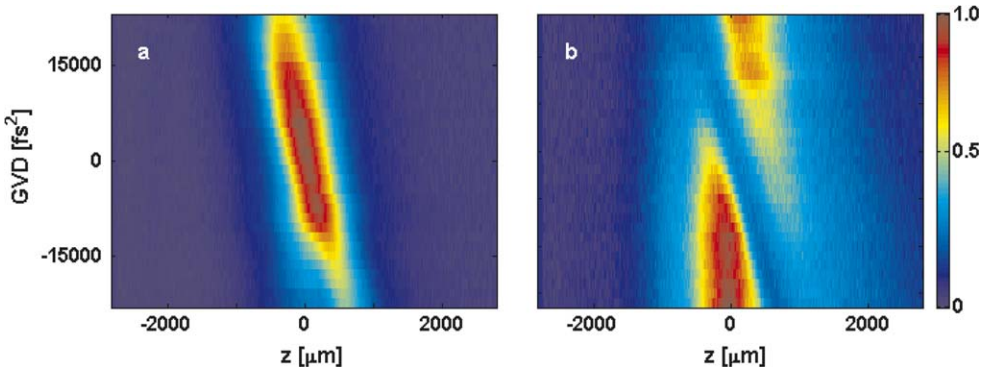

Fig. 4. Electronic Control of the location of the dark focus, by applying both a phase function leading to a dark focus at $z = 0$, and an arbitrary amount of additional GVD. We summarize the results of this experiment on a 2D plot, where each image was integrated along the axis perpendicular to the propagation direction. The horizontal axis shows the spatial coordinate along the propagation axis, whereas the vertical coordinate shows the amount of GVD applied by the SLM. (a) shows the results for GVD only, representing the shift of the focal plane as a function of the applied GVD. (b) shows the combined effect of a dark pulse and GVD, to form a dark nonlinear focus at a controlled coordinate along the propagation axis.

images show a dark region at $z = 0$ flanked on both sides by brighter regions. In the case where the π phase-step location exactly coincides with half the transition frequency, the transform-limited result is nearly reproduced, as predicted by Eq. (1).

We now turn to show how the location of the dark focus can be electronically controlled. To do so, we use the SLM to apply both a phase function leading to a dark focus at $z = 0$, and an arbitrary amount of additional chirp. We summarize the results of this experiment on a 2D plot, where each image was integrated along the axis perpendicular to the propagation direction. Thus, the horizontal axis of Fig. 4 shows the spatial coordinate along the propagation axis, whereas the vertical coordinate shows the amount of chirp applied by the SLM. Fig. 4(a) shows the results for chirp only, representing the shift of the focal plane as a function of the applied chirp, and Fig. 4(b) shows the combined effect of a dark pulse and chirp, to form a dark nonlinear focus at a controlled coordinate along the propagation axis. From these we can extract the geometric chirp rate of our setup due to temporal focusing by $45\left[\frac{fs^2}{\mu m}\right]$, in good correspondence with the expected value from a linear analysis [22].

5. Conclusion

In this work, we have demonstrated how the multiphoton excitation volume of temporally focused pulses can be manipulated by the use of pulse shaping techniques. In particular, we introduced the concept of a dark nonlinear focus, and demonstrated it experimentally.

Our experimental observation technique enabled us to directly visualize of the evolution of temporally focused pulses along the propagation axis by monitoring the atomic TPA rate. When combined with excitation by shaped pulses this visualization technique directly confirms our capability to exert control over the excitation volume.

Such spatio-temporal control of quantum-mechanical processes may find application in several areas where spatial control along the propagation length is required. Two such fields are atom manipulation and microscopy. In atom manipulation, and specifically in atom trapping, one use optical fields to form spatially modulated potentials. While it is simple to shape two-dimensional light patterns, the third-dimension is usually dictated by diffraction. Temporal focusing could be useful for modulating and controlling the potentials along the optical axis [2], although, for atomic manipulation, a much finer control on frequency might be necessary. In microscopy, nonlinear processes have been used to enhance optical contrasts and depth resolution. In particular, pulse shaping has been shown to control two- and three-photon fluorescence excitation microscopy [23]. It is possible to combine these techniques, together with the capability we have reported earlier [17,18], to improve depth resolution in two-photon microscopy. More specifically, it is conceivable that the dark focus demonstrated here might be used, in analogy with STED microscopy [1], to improve the resolution of nonlinear microscopy by depletion. We note that one interesting advantage of temporal dark focusing is that it can extend over an entire x–y plane, in contrast with a spatial dark focus that forms at a single point.

Acknowledgements

Financial support from the Israel Science Foundation and from the Horowitz Foundation is gratefully acknowledged.

References

[1] V. Westphal, S.W. Hell, Phys. Rev. Lett. 94 (2005) 143903.
[2] R. Ozeri, L. Khaykovich, N. Davidson, Phys. Rev. A 59 (1999) R1750.
[3] D. Meshulach, Y. Silberberg, Nature 396 (1998) 239.
[4] A.M. Weiner, D.E. Leaird, G.P. Wiederrecht, K.A. Nelson, J. Opt. Soc. Am. B 8 (1991) 1264.
[5] A. Assion, T. Baumert, M. Bergt, T. Brixner, B. Kiefer, V. Seyfried, M. Strehle, G. Gerber, Science 282 (1998) 919.
[6] A.M. Weiner, Rev. Sci. Instrum. 71 (2000) 1929.

[7] D. Felinto, L.H. Acioli, S.S. Vianna, Opt. Lett. 25 (2000) 917;
N. Dudovich, D. Oron, Y. Silberberg, Phys. Rev. Lett. 88 (2002) 123004.
[8] T. Feurer, J.C. Vaughan, K.A. Nelson, Science 299 (2003) 374.
[9] D. Oron, Y. Silberberg, Opt. Express 13 (2005) 9903.
[10] D. Meshulach, Y. Silberberg, Phys. Rev. A 60 (1999) 1287.
[11] S. Zamith et al., Phys. Rev. Lett. 87 (2001) 033001.
[12] J. Degert, W. Wohlleben, B. Chatel, M. Motzkus, B. Girard, Phys. Rev. Lett. 89 (2002) 203003.
[13] N. Dudovich, D. Oron, Y. Silberberg, Phys. Rev. Lett. 92 (2004) 103003.
[14] N. Dudovich, T. Polack, A. Peer, Y. Silberberg, Phys. Rev. Lett. 94 (2005) 083002.
[15] N. Dudovich, D. Oron, Y. Silberberg, Nature 418 (2002) 512.
[16] M. Renard, E. Hertz, B. Lavorel, O. Faucher, Phys. Rev. A 69 (2004) 043401.
[17] D. Oron, E. Tal, Y. Silberberg, Opt. Express 13 (2005) 1468.
[18] E. Tal, D. Oron, Y. Silberberg, Opt. Lett. 30 (2005) 1686.
[19] G. Zhu, J. van Howe, M. Durst, W. Zipfel, C. Xu, Opt. Express 13 (2005) 2153.
[21] E.B. Treacy, IEEE J. Quantum Electron. 5 (1969) 454.
[22] O.E. Martinez, IEEE J. Quantum Electron. 396 (1987) 239.
[23] J.P. Ogilvie, D. Debarre, X. Solinas, J.L. Martin, E. Beaurepaire, M. Joffre, Opt. Express 14 (2006) 759.